Published in : Brain : A Journal of Neurology (2008), vol. 131, pp. 381-388
Status : Postprint (Author's version)

Chromosomal profiles of gene expression in Huntington's disease

Alexander N. Anderson,[1] Federico Roncaroli,[2] Angela Hodges,[3] Manuel Deprez[4] and Federico E. Turkheimer[1,2]

[1]MRC Clinical Sciences Centre, Hammersmith Hospital, London, [2]Department of Clinical Neuroscience, Division of Neuroscience & Mental Health, Imperial College London, [3]MRC Centre for Neurodegeneration Research, Institute of Psychiatry, London, UK and [4]Laboratory of Neuropathology Department of Pathology, University Hospital of Liège, Belgium

Abstract

Recent studies suggested that Huntington's disease is due to aberrant interactions between mutant huntingtin protein, transcription factors and transcriptional co-activators resulting in widespread transcriptional dysregulation. Mutant huntingtin also interacts with histone acetyltransferases, consequently interfering with the acetylation and deacetylation states of histones. Because histone modifications and chromatin structure coordinate the expression of gene clusters, we have applied a novel mathematical approach, *Chromowave*, to analyse microarray datasets of brain tissue and whole blood to understand how genomic regions are altered by the effects of mutated huntingtin on chromatin structure. Results show that, in samples of caudate and whole blood from Huntington's disease patients, transcription is indeed deregulated in large genomic regions in coordinated fashion, that transcription in these regions is associated with disease progression and that altered chromosomal clusters in the two tissues are remarkably similar. These findings support the notion of a common genome-wide mechanism of disruption of RNA transcription in the brain and periphery of Huntington's disease patients.

Keywords : Huntington's disease ; microarrays ; histone deacetylase ; chromosomal expression ; Chromowave

Abbreviations : HD = Huntington's disease ; HDAC = histone deacetylase

INTRODUCTION

Huntington's disease (HD) is an autosomal-dominant neurodegenerative disorder caused by expansion of the CAG repeat region in exon 1 of the HD gene on 4p16 that encodes for the protein huntingtin. Such expansion results in abnormal polyglutamine repeats at the N-terminus of huntingtin (Walker, 2007) that cannot be cleaved by caspase 3 (Hermel *et al.*, 2004). The mechanisms leading to huntingtin-mediated cell toxicity are still unresolved although it is clear that the mutated protein affects multiple pathways causing cell death.

Mutated huntingtin has been shown to interfere with the transcriptional machinery of the cell. The N-terminal fragments aggregate and sequester several transcription factors leading to decreased availability for binding to DNA promoter regions, and consequent decrease in transcription (Chen-Plotkin *et al.*, 2006). Recent studies in HD models have also shown that mutated huntingtin interferes with the activity of histone acetyltransferase, suggesting that abnormal activity of this enzyme might be a cause of transcriptional dysregulation in HD (Steffan *et al.*, 2001; Sadri-Vakili and Cha, 2006). This observation is supported by the effect of histone deacetylase (HDAC) inhibitors in a number of HD models (Butler and Bates, 2006).

Eukaryotic DNA is wrapped around histones to form chromatin. Nucleosomes, the basic units of chromatin, are composed of eight histones and are arranged to form a structure that facilitates the packaging of chromatin. The transition between tightly protected chromatin to freely accessible DNA is controlled, in part, by modification of the tails of histone proteins. These tails may be modified by adding acetyl groups, phosphates, methyl groups, adenosine diphosphate molecules or ubiquitin proteins (Kuo and Allis, 1998; Cheung *et al.*, 2000; Kouzarides, 2002; Gill, 2004). Acetylation is an important part of the histone-modification code (Kuo and Allis, 1998) because DNA is released by removing the positive charges of the histories through the acetylation of the lysine residues. This results in the loosening of the tightly packed chromatin with subsequent greater access to the DNA by transcription factors and RNA polymerase. The alleged interference of mHtt with histone acetylation is therefore expected to affect transcription globally (Fig. 1).

Since it is thought to affect the acetylation state of histones and, thus, chromatin structure that coordinates the expression of gene clusters, we hypothesized that (i) mutated huntingtin affects the transcription of large

chromosomal domains, (ii) that the effect of mutated huntingtin is similar in different body tissues and (iii) that chromosomal expression profiles are associated with the disease state. These hypotheses were tested using the genome-scale mRNA measurements of HD tissue available at the time of the project. These consisted in one large microarray study of whole blood in a series of patients and controls (Borovecki *et al.*, 2005) and in a second microarray study of postmortem brain tissue from patients and controls (Hodges *et al.*, 2006). We then processed the datasets with *Chromowave*, a microarray processing tool that allows the identification, with high specificity, of clusters of adjacent genes with homogeneous changes of expression and maps their position on chromosomes (Turkheimer *et al.*, 2006).

Fig. 1 *Histone acetylation is generally linked to transcriptional activation. Histone acetyltransferases (HATs) acetylate lysine residues at the N-terminals of histone proteins, resulting in a loosely packed chromatin structure in which DNA promoter regions are more accessible to transcription factors. Conversely, histone deacetylation, catalysed by histone deacetylases (HDACs), leads to a tightly packed chromatin structure, corresponding to transcriptional repression. Transcriptional repression also occurs when mHtt interacts with HATs, leading to a decrease in the acetylation of histone proteins.*

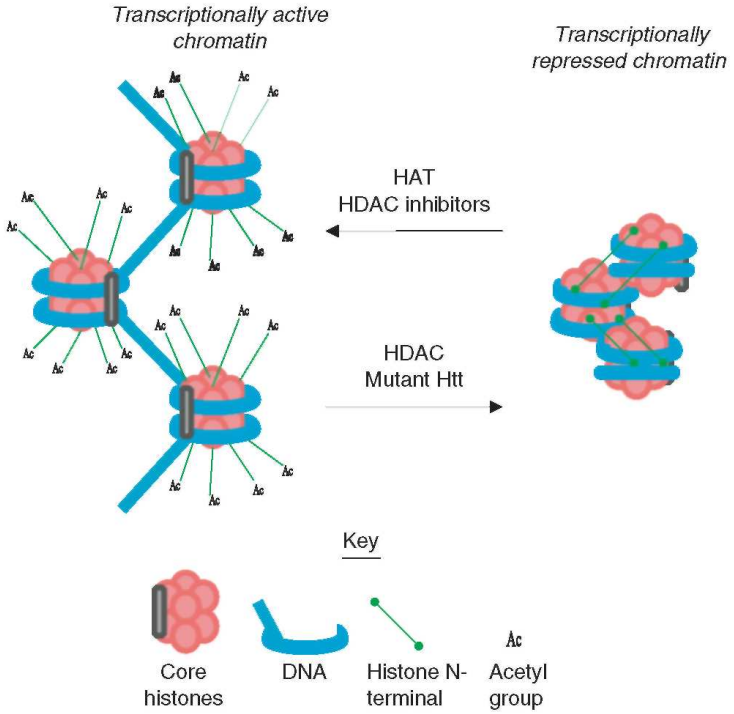

METHODS

Microarray data

The microarray dataset that analysed global gene expression in blood samples of HD patients, matched controls and pre-symptomatic subjects was taken from a published study that used Affymetrix and Amersham Biosciences oligonucleotide microarrays (Borovecki *et al.*, 2005) and is available from the GEO database. Unfortunately, because of the unavailability of genome alignment data of the Amersham CodeLink arrays, only the data from the Affymetrix platform could be used (series accession GSE1751, platform Affymetrix GeneChip HG-U133A). The set contained $n = 14$ controls, $n = 12$ HD samples plus $n = 5$ samples from subjects with genetically determined disease but no overt clinical symptoms. The second dataset consisted in samples of caudate nucleus ($n = 14$ controls, $n = 15$HD), frontal cortex ($n = 12$ controls, $n = 17$HD) and cerebellum ($n = 11$ controls, $n = 17$HD) of genetically confirmed HD patients and age-and sex-matched normal subjects. The dataset is deposited at the Array Express Repository (Experiment E-AFMX-6, platform Affymetrix GeneChip HG-U133A and HG-U133B).

Published in : Brain : A Journal of Neurology (2008), vol. 131, pp. 381-388
Status : Postprint (Author's version)

Chromowave analysis

Chromowave (Turkheimer *et al.*, 2006) (written in MATLAB 6.5, the Mathworks Inc., Natick MA, USA) normalized the microarrays to the background by dividing intensities by the median value of those genes presented with positive detection. Expression values were then log2 transformed, mapped to their corresponding chromosomal location using the genome alignment information contained in the manifest of each platform (available at http:// www.affymetrix.com/support/technical/manual/taf_manual.affx).

Chromowave then applied the wavelet transform to the spatial distribution of the probes and converted the original expression values to wavelet coefficients that are functions of the expression of adjacent genes. Unlike the Fourier transform, that is the classical operator for stationary (periodic) signals, wavelets are a recently introduced mathematical tool for the treatment of signals with 'non-periodical behaviour' (e.g. a hammer blow, a plane flyover noise, etc.). Their use is pervasive in areas such as data encoding, transmission and compression including the analysis of gene sequences and functional genomics data (Lio, 2003).

The wavelet transform is an orthogonal mathematical operator which means that the noise level is identical on the original raw data and at all wavelet transform levels. This is advantageous because a cluster of genes with similar expression is transformed into a wavelet transform coefficient that is greater the larger the number of genes in the cluster. Therefore the net effect of the application of the wavelet transform is that genes with individual expression below the noise level, that would otherwise go undetected, are identified when clustered together because their combined energy condenses into a greater wavelet coefficient that arises over the noise.

Unsupervised extraction of chromosomal profiles

The genome-wide ensemble of wavelet coefficients can be used for traditional ways of statistical analysis. In this instance we were interested in extracting the main pattern of chromosomal variation across each of the two datasets, irrespective of the grouping, and to verify *afterwards* whether major chromosomal variation was indeed associated with the disease state (e.g. unsupervised analysis).

The choice of unsupervised analysis instead of a group comparison was consequential to the hypotheses to be tested. The first hypothesis stated that mutated huntingtin interference would cause a major disruption of the chromatin regulation of RNA. Unsupervised analysis (factor analysis in the instance considered here) allows the identification and quantification (in terms of percentage of total variability) of the major pattern of variation in a data-set. Factor analysis also allows the extraction of subject loadings that can be used in a regression model to verify the association of the pattern extracted from the data with disease states. Finally, one basic assumption of group analysis is that groups need to be homogeneous, clearly not the case in the instance of the data considered in this work.

For this purpose, *Chromowave* applied the singular value decomposition to the set of wavelet coefficients to extract the first eigenvector, e.g. the main pattern of variation. This pattern was subsequently filtered using a highly conservative threshold that accounted for statistical noise, the number of wavelets and the probe-probe genomic distance; note that in *Chromowave* the contribution of the individual probes (wavelet transform coefficients at the first level) is zeroed so that only coherent spatial variation of expression is detected. After filtering, the surviving set of coefficients was then passed into the inverse wavelet transform to generate the genome-wide pattern of variation. The contribution of each array to the pattern was calculated as a single number, the 'case loading', where a positive value indicates an increased pattern of expression compared to a negative value indicating that a lower pattern is expressed.

Analysis of individual probes expression

In order to verify some of the findings with *Chromowave*, we also performed traditional probe-by-probe statistical analysis. The normalized expression values were log2 transformed and then a Student *t*-test was applied to identify differentially expressed genes between groups. The P-values were then corrected for the number of multiple comparisons using the false discovery rate criterion (Reiner *et al.*, 2003) where this was fixed at 5%.

Published in : Brain : A Journal of Neurology (2008), vol. 131, pp. 381-388
Status : Postprint (Author's version)

RESULTS

Analysis of blood samples

The main pattern of chromosomal variation (40% of total variance) obtained from the dataset of blood samples clearly distinguished controls and HD cases ($P < 0.000001$, Mann-Whitney test) as well as controls and preclinical HD ($P = 0.0003$, Mann-Whitney test). The distinction between preclinical and clinically manifested HD was less sharp ($P = 0.06$, Mann-Whitney test), likely because of the low number of preclinical cases (Fig. 2). Large-scale clusters of co-expressed genes appeared to be up-regulated or down-regulated against controls (Fig. 3). Some localized clusters are of interest. One that is considerably down-regulated is on Chr1.p36-p35 and contains *MTHFR*, *CASP9*, *DFFB*, *FRAP1* and *SHDB* genes that have been linked to HD (Kiechle *et al.*, 2002; Brune *et al.*, 2004; Ravikumar *et al.*, 2004; Chattopadhyay *et al.*, 2005; Majumder *et al.*, 2006). Among these genes, only *MTHFR* individual expression was significantly down-regulated and passed false discovery rate multiple correction (mean expression ratio HD versus controls = 0.55, $P = 0.0037$). The repressed cluster on Chr6p21-23 has been previously implicated in the age at onset of HD (Li *et al.*, 2003) (Fig. 3).

Analysis of post-mortem tissues

The case loadings of the main chromosomal pattern (51% of total variance) obtained with the post-mortem tissues caudate samples demonstrate a significant difference between Hd cases and controls ($P = 0.00014$, Mann-Whitney test) (Fig. 4). In addition, a Spearman's test found significant positive correlation between HD pathological grade and mRNA expression profile ($P = 0.017$) where the severity of the disease was graded according to the Vonsattel classification scale (Vonsattel *et al.*, 1985). Inspection of Fig. 4, illustrates that the pattern is markedly expressed in cases graded 2 and higher, less so in grades 0 and 1. *Chromowave* analysis of the arrays obtained from frontal and cerebellar samples did not result in any significant chromosomal profile. In caudate, the pattern also extends along large stretches of chromatin but at a lower intensity than the one observed in blood cells (Fig. 5).

Comparison between blood and post-mortem samples

Striking similarities between the two patterns, particularly involving the whole of Chr4, Chr5, Chr8, Chr10, Chr12, Chr19 and Chr20 are observed between blood and postmortem tissues (Fig. 6). For instance, note that both patterns contain localized groups of down-regulated genes in a telomeric region of ~8 MB of Chr4p around the HD gene confirming the involvement in the disease of genes on this region other than the HD (Farrer *et al.*, 1993; Li *et al.*, 2003; Djousse *et al.*, 2004).

Fig. 2 *Case loadings for blood sample datasets. HD patients (black bars, cases HDI-12), controls (white bars, cases NI-14) and pre-symptomatic patients (black bars, cases PI-5).*

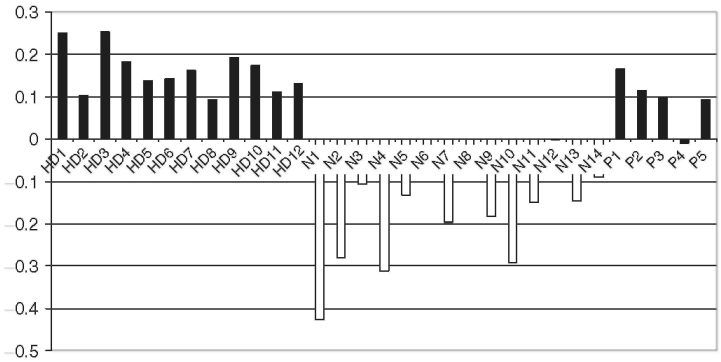

Published in : Brain : A Journal of Neurology (2008), vol. 131, pp. 381-388
Status : Postprint (Author's version)

Fig. 3 *Pattern of chromosomal expression extracted by Chromowave for blood sample datasets: x-axis represents the genomic distance along each of the chromosomes; y-axis represents the gene expression contribution (intensity and direction, log2 scale). Positive values depict up-regulation of mRNA expression in HD patients and down-regulation in controls.*

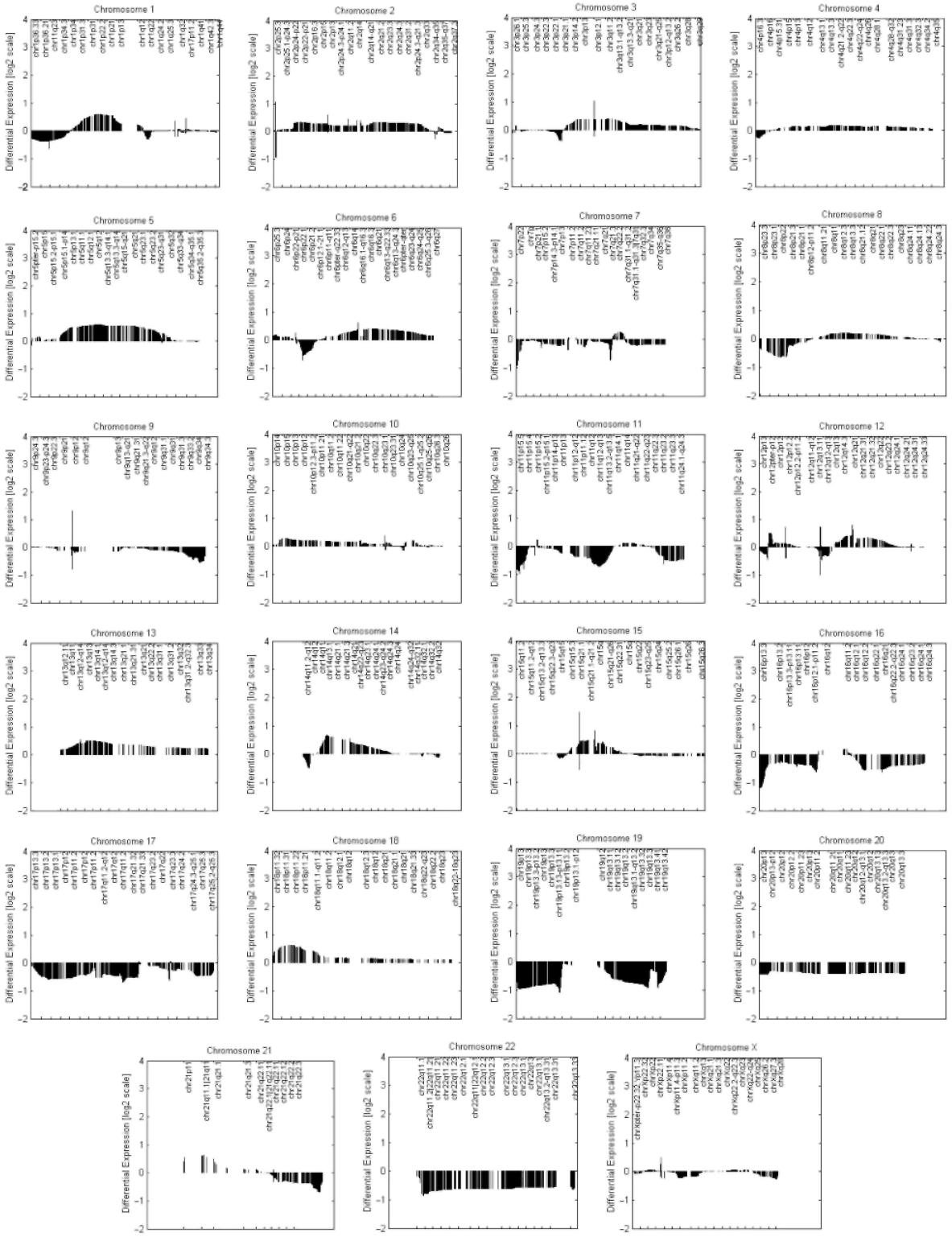

Published in : Brain : A Journal of Neurology (2008), vol. 131, pp. 381-388
Status : Postprint (Author's version)

Fig. 4 *Case loadings for caudate sample datasets (controls = white, HD patients = black, with numbers above plots indicating Vonsattel scale of disease pathology).*

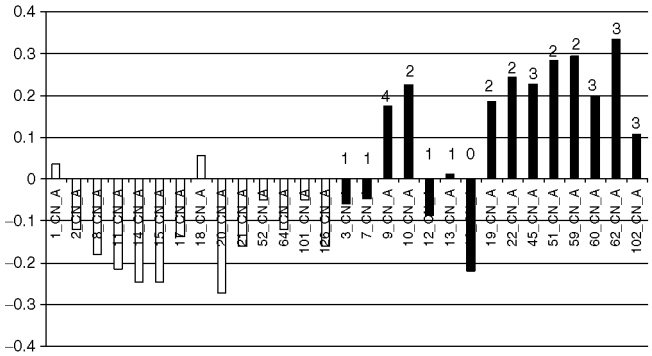

Published in : Brain : A Journal of Neurology (2008), vol. 131, pp. 381-388
Status : Postprint (Author's version)

Fig. 5 *Pattern of chromosomal expression extracted by Chromowave for caudate sample datasets: x-axis represents the genomic distance along each of the chromosomes; y-axis represents the gene expression contribution (intensity and direction, log2 scale). Positive values depict up-regulation of mRNA expression in HD patients and down-regulation in controls.*

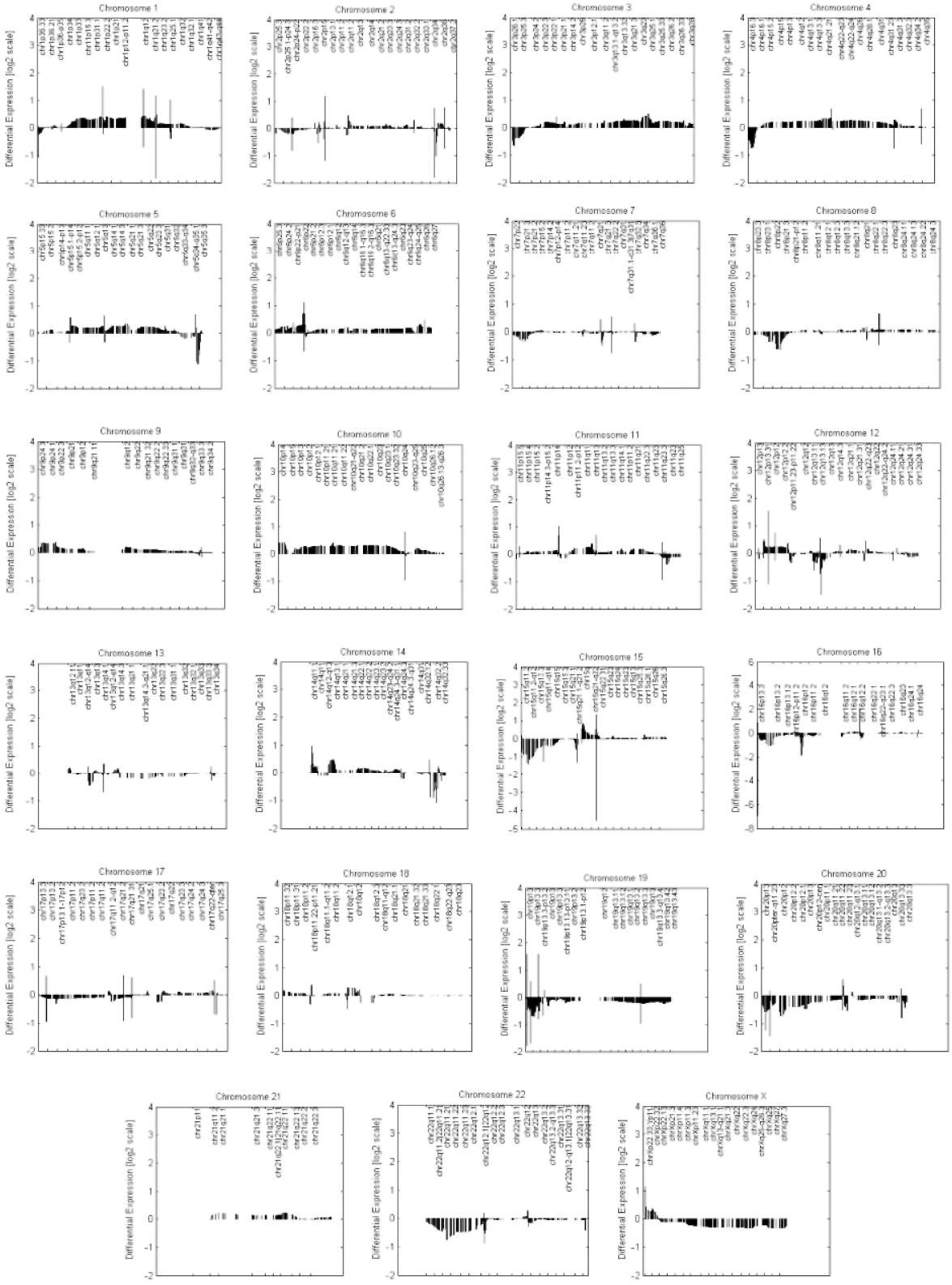

Published in : Brain : A Journal of Neurology (2008), vol. 131, pp. 381-388
Status : Postprint (Author's version)

Fig. 6 *Side-by-side comparison of the six chromosomal profiles (chr4, chr5, chr8, chr10, chr19, chr20) with the highest similarity between blood and striatum: x-axis represents the genomic distance along each of the chromosomes; y-axis represents the gene expression contribution (intensity and direction, log2 scale).*

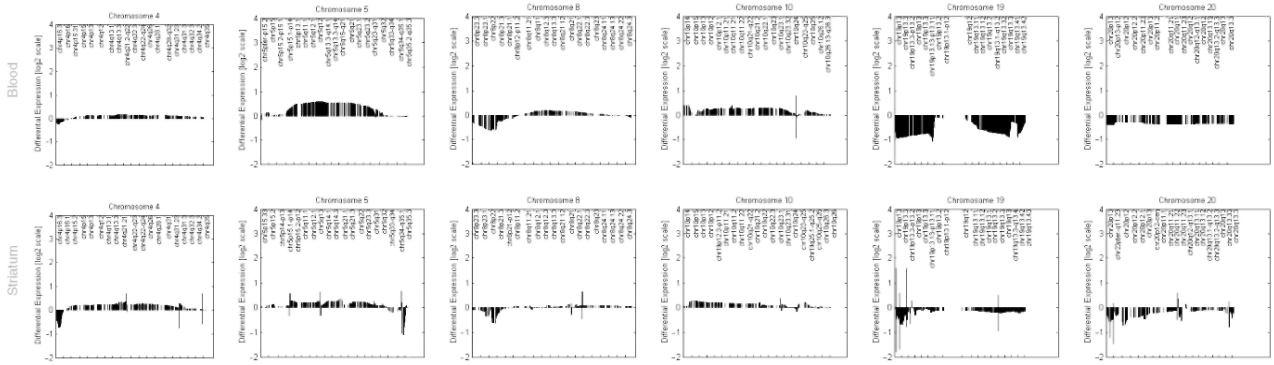

Individual probes analysis

In both datasets, a very large number of transcripts displayed significant change and survived the false discovery rate correction. Both original references (Borovecki *et al.*, 2005; Hodges *et al.*, 2006) contain exhaustive lists of these individual transcripts. Here we focus on the sub-set of genes that showed the largest up/down-regulation in those chromosomal locations identified by *Chromowave* and whose deregulation was consistent in both blood and striatum. This set, listed in Table 1, contains the DRD2 receptor gene, the hallmark of movement disorders, and genes vital to calcium homeostasis (NRGN, TRPM2, CACNA1A, CACNG4), G-protein signalling (RGS4, HRAS), exocytosis (EXOC7, VAMP2) and endocytosis (DNM1). Of interest is also the up-regulation of genes that induce apoptosis (FAS), transducers of Interleukin6 (IL6ST), whose levels are increased in the plasma of HD patients (Dalrymple *et al.*, 2007), and the down-regulation of dynamin synaptic proteins (DNM1) previously involved in the disease (DiProspero *et al.*, 2004).

Published in : Brain : A Journal of Neurology (2008), vol. 131, pp. 381-388
Status : Postprint (Author's version)

Table 1 *Transcripts with major up/down regulation, consistent in both blood and striatum (striatal values in grey shading)*

Probe set name	Mean ratio	P value	Gene symbol	Location	Descriptor
204338.s.at	0.41	0.0028	RGS4	chr1q23.3	Regulator of G-protein signalling
	0.71	0.0041			
203138.at	2.58	0.0007	HATI	chr2q31.2	Histone acetyltransferase 1
	1.15	0.0034			
200982.s.at	3.57	<0.0001	IL6ST	chr5q11	Interleukin 6 signal transducer
	1.33	0.001			
201255.x.at	0.57	<0.0001	BAT3	chr6p21.3	HLA-B associated transcript
	0.87	0.0006			
215116.s.at	0.54	0.002	DNMI	chr9q34	Dynamin 1
	0.54	0.0001			
204781.s.at	2.31	<0.0001	FAS	chr10q24.1	Fas (TNF receptor superfamily, member 6)
	1.19	0.0002			
212983.at	0.70	0.0033	HRAS	chr11p15.5	v-Ha-ras Harvey rat sarcoma viral oncogene homolog
	0.70	0.0002			
216938.x.at	0.59	0.0047	DRD2	chr11q23	Dopamine receptor D2
	0.62	<0.0001			
204081.at	0.60	0.0012	NRGN	chr11q24	Neurogranin (protein kinase C substrate, RC3)
	0.39	<0.0001			
214792.x.at	0.58	0.004	VAMP2	chr17p13.1	Vesicle-associated membrane protein 2
	0.69	0.0003			
62987.r.at	0.52	0.0033	CACNG4	chr17q24	Calcium channel, voltage- dependent, gamma sub 4
	0.62	<0.0001			
211997.x.at	1.49	0.0011	H3F3B	chr17q25	H3 histone, family 3B
	1.44	0.0007			
212034.s.at	0.71	0.0003	EXOC7	chr17q25.1	Exocyst complex component 7
	0.88	0.0035			
208255.s.at	0.50	0.0004	FKBP8	chr19p12	FK506 binding protein 8
	0.76	0.0001			
218522.s.at	0.55	0.001	MAPIS	chr19p13.11	Microtubule-associated protein IS
	0.85	0.0001			
221506.s.at	0.48	0.0047	TNP02	chr19p13.13	Transportin 2 (importin 3, karyopherin beta 2b)
	0.86	0.0075			
210770.s.at	0.44	0.0012	CACNAIA	chr19p13.2	Calcium channel, voltage- dependent, alpha IA subunit
	0.78	<0.0001			
205708.s.at	0.74	0.0056	TRPM2	chr21q22.3	Transient receptor potential cation channel
	0.79	0.0004			
205013.s.at	0.50	0.0005	ADORA2A	chr22q 11.23	Adenosine A2a receptor
	0.48	<0.0001			

The mean ratio is calculated as the ratio of the mean expression in the HD and the mean expression in the control group.

DISCUSSION

The results extracted by Chromowave using two previously published expression microarray datasets supported the view that coordinated repression and expression of large chromosomal regions may explain the pathogenetic mechanism that underlie HD (Borovecki *et al.*, 2005; Hodges *et al.*, 2006). The transcriptional repression of these regions is consistent with the effect of mHtt on the acetylation state of histones and the consequent compaction of chromatin regions (Butler and Bates, 2006; Sadri-Vakili and Cha, 2006). Notably, the effect size of the transcriptional changes, particularly in the whole blood samples, was comparable to the mRNA down-regulation previously observed in a set of low grade and anaplastic gliomas (Turkheimer *et al.*, 2006) where marked reduction in expression was secondary to loss of genetic material, as proved with FISH analysis but also

to epigenetic control.

Interestingly, transcriptional changes were quite evident in the blood samples of pre-clinical HD subjects (4/5 were outside the normal range) but this finding was not replicated in the caudate samples of subjects at the low end of the Vonsattel scale. The latter result however may be due to the lower quality of RNA in post-mortem samples.

In the analysed samples, the observed large domains of repressed transcription co-exist with sizeable domains of increased transcription. The increased activity of a large number of transcripts, that has been previously reported (Borovecki *et al.*, 2005; Hodges *et al.*, 2006), can be also explained with the particular chromosomal model adopted here. For example, in the dataset from blood samples of HD patients the repressed regions Chr1p34, Chr17q21 and ChrXp11.2 contain HDAC genes (HDAC1, HDAC5 and HDAC6, respectively) whose inactivation could result in increased acetylation of the relative histones and local increases in transcription. Also, the increased transcription observed in some chromosomes can be explained by the changes in cell population within the affected tissue (i.e. astrocytosis and microglial activation associated with nerve cell loss). For instance, the chromosomal region chr6p, which shows repressed transcription in the blood cells of HD samples is largely active in the HD striatal samples, likely because of the presence of microglial activity in caudate of HD patients (Sapp *et al.*, 2001) and whose transcriptional signature contains MHC molecules, which are encoded by genes on Chr6p (Horton *et al.*, 2004). Individual probe analysis of the microarray data for the caudate samples confirmed up-regulation of MHC Class I molecules but not of MHC Class II nor tumour necrosis factors, interleukins (IL 1-33) or interferon (type 1-3) (data not shown).

The observation of large congruencies between chromosomal profiles in blood and brain tissue samples validates further the hypothesis that the mechanism of interference of mutated huntingtin with histone acetyltransferases generates a similar pattern of transcriptional repression in tissues that are affected by the disease. Furthermore, the similarities between the expression profiles in blood and tissue samples identify the genes that are involved in the pathogenesis of HD. The most striking similarities are observed in chr4, chr8, chr10, chr12, chr19 and chr20 where changes in expression extend throughout the chromosome. In other chromosomes such as chr5, chr14, chr15, chr16, chr17 and chr22 and chrX the correspondence between blood and tissue is more limited but still extends to or more than 50% of the chromatin.

Finally, the significant association between genome-wide patterns extracted with *Chromowave* and clinical progression brings quantitative evidence to the suggestion made by Borovecki *et al.* (2005) that analysis of peripheral blood samples can provide a minimally non-invasive and easily accessible approach to monitor disease progression and therapy efficacy in HD patients. In particular, chromosomal patterns of expression from microarray peripheral data are promising tools for the assessment of biological efficacy of histone deacetylase inhibitors (Butler and Bates, 2006).

In conclusion, this is the first time that the putative large-scale effects of mutated huntingtin on global changes in gene expression have been visualized in peripheral blood and brain tissue. The ability of *Chromowave* of detecting expression changes of gene clusters and map their position on chromosomes allowed a step forward in understanding the widespread effects of mutated huntingtin on the human genome.

References

Borovecki F, Lovrecic L, Zhou J, et al. Genome-wide expression profiling of human blood reveals biomarkers for Huntington's disease. Proc Natl Acad Sci USA 2005; 102: 11023-8.

Brune N, Andrich J, Gencik M, et al. Methyltetrahydrofolate reductase polymorphism influences onset of Huntington's disease. J Neural Transm Suppl 2004; 105-10.

Butler R, Bates GP. Histone deacetylase inhibitors as therapeutics for polyglutamine disorders. Nat Rev Neurosci 2006; 7: 784-96.

Chattopadhyay B, Baksi K, Mukhopadhyay S, Bhattacharyya NP. Modulation of age at onset of Huntington disease patients by variations in TP53 and human caspase activated DNase (hCAD) genes. Neurosci Lett 2005; 374: 81-6.

Chen-Plotkin AS, Sadri-Vakili G, Yohrling GJ, et al. Decreased association of the transcription factor Sp1 with genes downregulated in Huntington's disease. Neurobiol Dis 2006; 22: 233-41.

Cheung P, Allis CD, Sassone-Corsi P. Signaling to chromatin through histone modifications. Cell 2000; 103: 263-71.

Dalrymple A, Wild EJ, Joubert R, et al. Proteomic profiling of plasma in Huntington's disease reveals neuroinflammatory activation and biomarker candidates. J Proteome Res 2007; 6: 2833-40.

DiProspero NA, Chen EY, Charles V, Plomann M, Kordower JH, Tagle DA. Early changes in Huntington's disease patient brains involve alterations in cytoskeletal and synaptic elements. J Neurocytol 2004; 33: 517-33.

Djousse L, Knowlton B, Hayden MR, et al. Evidence for a modifier of onset age in Huntington disease linked to the HD gene in 4p16. Neurogenetics 2004; 5: 109-14.

Farrer LA, Cupples LA, Wiater P, Conneally PM, Gusella JF, Myers RH. The normal Huntington disease (HD) allele, or a closely linked gene, influences age at onset of HD. Am J Hum Genet 1993; 53: 125-30.

Gill G. SUMO and ubiquitin in the nucleus: different functions, similar mechanisms? Genes Dev 2004; 18: 2046-59.

Hermel E, Gafni J, Propp SS, et al. Specific caspase interactions and amplification are involved in selective neuronal vulnerability in Huntington's disease. Cell Death Differ 2004; 11: 424-38.

Hodges A, Strand AD, Aragaki AK, et al. Regional and cellular gene expression changes in human Huntington's disease brain. Hum Mol Genet 2006; 15: 965-77.

Horton R, Wilming L, Rand V, et al. Gene map of the extended human MHC. Nat Rev Genet 2004; 5: 889-99.

Kiechle T, Dedeoglu A, Kubilus J, et al. Cytochrome C and caspase-9 expression in Huntington's disease. Neuromolecular Med 2002; 1: 183-95.

Kouzarides T. Histone methylation in transcriptional control. Curr Opin Genet Dev 2002; 12: 198-209.

Kuo MH, Allis CD. Roles of histone acetyltransferases and deacetylases in gene regulation. Bioessays 1998; 20: 615-26.

Li JL, Hayden MR, Almqvist EW, et al. A genome scan for modifiers of age at onset in Huntington disease: the HD MAPS study. Am J Hum Genet 2003; 73: 682-7.

Lio P. Wavelets in bioinformatics and computational biology: state of art and perspectives. Bioinformatics 2003; 19: 2-9.

Majumder P, Chattopadhyay B, Mazumder A, Das P, Bhattacharyya NP. Induction of apoptosis in cells expressing exogenous Hippi, a molecular partner of huntingtin-interacting protein Hipl. Neurobiol Dis 2006; 22: 242-56.

Ravikumar B, Vacher C, Berger Z, et al. Inhibition of mTOR induces autophagy and reduces toxicity of polyglutamine expansions in fly and mouse models of Huntington disease. Nat Genet 2004; 36: 585-95.

Reiner A, Yekutieli D, Benjamini Y. Identifying differentially expressed genes using false discovery rate controlling procedures. Bioinformatics 2003; 19: 368-75.

Sadri-Vakili G, Cha JH. Mechanisms of disease: Histone modifications in Huntington's disease. Nat Clin Pract Neurol 2006; 2: 330-8.

Sapp E, Kegel KB, Aronin N, et al. Early and progressive accumulation of reactive microglia in the Huntington disease brain. J Neuropathol Exp Neurol 2001; 60: 161-72.

Steffan JS, Bodai L, Pallos J, et al. Histone deacetylase inhibitors arrest polyglutamine-dependent neurodegeneration in Drosophila. Nature 2001; 413: 739-43.

Turkheimer FE, Roncaroli F, Hennuy B, et al. Chromosomal patterns of gene expression from microarray data: methodology, validation and clinical relevance in gliomas. BMC Bioinformatics 2006; 7: 526.

Vonsattel JP, Myers RH, Stevens TJ, Ferrante RJ, Bird ED, Richardson EP Jr. Neuropathological classification of Huntington's disease. J Neuropathol Exp Neurol 1985; 44: 559-77.

Walker FO. Huntington's disease. Lancet 2007; 369: 218-28.